Electronic Supplementary Material (ESI) for Green Chemistry.
This journal is © The Royal Society of Chemistry 2024

Electronic Supplementary Information

Counter-current chromatography for lignin monomer-monomer and monomer-oligomer separations from reductive catalytic fractionation oil

Hoon Choi,[†] Manar Alherech,[†] Jun Hee Jang,[¶] Sean P. Woodworth, Kelsey J. Ramirez, Eric M. Karp,[‡] Gregg T. Beckham*

Renewable Resources and Enabling Sciences Center, National Renewable Energy Laboratory, Golden, CO 80401, USA
[†] Equal contribution
[¶] Current address: Department of Chemical Engineering, Rowan University, Glassboro, New Jersey 08028, United States
[‡] Current address: Crysalis BioSciences Inc., Louisville CO, USA 80201
* Corresponding author: gregg.beckham@nrel.gov

Table S1. HEMWat solvent system composition[1]

Solvent System	Hexane	Ethyl Acetate	Methanol	Water	Average Polarity
HEMWat -7	9	1	9	1	3.07
HEMWat -6	8	2	8	2	3.54
HEMWat -5	7	3	7	3	4.01
HEMWat -4	7	3	6	4	4.27
HEMWat -3	6	4	6	4	4.48
HEMWat -2	7	3	5	5	4.52
HEMWat -1	6	4	5	5	4.74
HEMWat 0	5	5	5	5	4.95
HEMWat +1	4	6	5	5	5.16
HEMWat +2	3	7	5	5	5.38
HEMWat +3	4	6	4	6	5.42
HEMWat +4	3	7	4	6	5.64
HEMWat +5	3	7	3	7	5.89
HEMWat +6	2	8	2	8	6.36
HEMWat +7	1	9	1	9	6.83
HEMWat +8	0	10	0	10	7.30

*the average polarity of the solvent system is calculated based on the solvent polarity index from Rohrschneider-Snyder classification[1]

**the solvent composition of the upper and lower phase of each solvent system can be found in Berthod *et al*.[2] Specifically, for the HEMWat -3 solvent system, the upper layer is approximately 0.2% water, 20.2% ethyl acetate, 76.3% hexane, and 3.3% methanol whereas the lower layer is approximately 32.1% water, 20.4% ethyl acetate, 0.5% hexane, and 47.0% methanol (v/v%).

Table S2. Monomer composition in the lignin oil substrates (wt% in oil) used in this study. RCF reaction conditions for poplar, pine, and corn stover: 3 g of feedstock, 0.3 g of 5 wt% Ru/C, 30 mL of methanol, and 30 bar H_2 at 225 °C for 3 hours after a 30 minute temperature ramp. RCF reaction conditions for propyl-rich poplar: 10 g of feedstock, 1 g of Pt/C (5 wt%), 150 mL of methanol/water (50:50 v/v), 225 °C, 1 bar of N_2 (at room temperature), and 3 hours after a 30 minute temperature ramp.

	Poplar		Pine		Corn Stover		Propyl-rich Poplar	
	(wt%)	STDEV	(wt%)	STDEV	(wt%)	STDEV	Wt.%	STDEV
propanol syringol	1.89%	0.34			1.47%	0.09	1.01%	0.29
propanol guaiacol	1.50%	0.09	3.52%	0.12	1.70%	0.07	0.88%	0.05
methyl paraben	2.83%	0.22	N.D.		N.D.		0.47%	0.16
methylhydro coumarate	N.D.		N.D.		8.18%	0.29	N.D.	
methylhydro ferulate	N.D.		N.D.		4.86%	0.16	N.D.	
methyl coumarate	N.D.		N.D.		2.12%	0.74	N.D.	
methyl ferulate	N.D.		N.D.		0.28%	0.03	N.D.	
ethyl syringol	0.45%	0.09	N.D.		N.D.		3.98%	0.08
ethyl phenol	N.D.		N.D.		3.52%	0.17	N.D.	
ethyl guaiacol	0.13%	0.06	0.63%	0.05	0.80%	0.00	1.92%	0.06
propenyl syringol	3.50%	0.24	N.D.		1.70%	0.03	N.D.	0.19
isoeugenol	2.31%	0.24	3.30%	0.13	1.20%	0.02	N.D.	0.19
propyl syringol	11.29%	1.33	0.00%		4.15%	0.09	17.29%	1.13
propyl guaiacol	7.27%	0.79	20.28%	0.47	2.81%	0.04	7.98%	0.67
TOTAL	32.05%		27.73%		33.01%		33.53%	

*N.D.: not determined.

Table S3. Log of partition coefficient ($\log_{10} K_P$) of each monomer in HEMWat solvent system from the shake flask test (Figure 3). The numbers in the parentheses denote the volume ratio of hexane, ethyl acetate, methanol, and water.

Hardwood

HEMWat	propanol syringol	propanol guaiacol	methyl paraben	ethyl guaiacol	isoeugenol	propyl syringol	propyl guaiacol
-5 (7/3/7/3)		-1.83	-0.94	-0.21	-0.20	-0.41	-0.01
-4 (7/3/6/4)	-1.93	-1.67	-0.65	0.10	0.13	-0.10	0.35
-3 (6/4/6/4)	-1.65	-1.27	-0.34	0.29	0.33	0.12	0.51
-2 (6/5/6/5)	-1.32	-0.95	-0.05	0.52	0.59	0.38	0.75
0 (5/5/5/5)	-1.08	-0.71	0.19	0.73	0.82	0.61	0.98
+2 (5/6/5/6)	-0.85	-0.48	0.42	0.92	1.03	0.80	1.17
+3 (4/6/4/6)	-0.57	-0.18	0.74	1.20	1.34	1.11	1.48

Softwood

HEMWat	propanol guaiacol	ethyl guaiacol	isoeugenol	propyl guaiacol			
-5 (7/3/7/3)	-1.82	-0.20	-0.19	0.00			
-4 (7/3/6/4)	-1.61	0.11	0.14	0.35			
-3 (6/4/6/4)	-1.24	0.31	0.35	0.53			
-2 (6/5/6/5)	-0.96	0.52	0.59	0.75			
0 (5/5/5/5)	-0.72	0.71	0.80	0.95			
+2 (5/6/5/6)	-0.48	0.93	1.04	1.19			
+3 (4/6/4/6)	-0.23	1.15	1.27	1.40			

Grasses

HEMWat	propanol syringol	propanol guaiacol	methylhydro coumarate	methylhydro ferulate	ethyl phenol	ethyl guaiacol	isoeugenol	propyl syringol	propyl guaiacol
-5 (7/3/7/3)		-1.78	-0.96	-0.88	-0.28	-0.21	-0.21	-0.41	-0.01
-4 (7/3/6/4)		-1.64	-0.67	-0.61	0.05	0.10	0.12	-0.09	0.34
-3 (6/4/6/4)	-1.48	-1.24	-0.34	-0.32	0.27	0.27	0.30	0.10	0.48
-2 (6/5/6/5)	-1.29	-0.93	-0.01	-0.03	0.57	0.53	0.60	0.39	0.77
0 (5/5/5/5)	-1.01	-0.66	0.24	0.20	0.79	0.73	0.82	0.62	1.00
+2 (5/6/5/6)	-0.79	-0.43	0.46	0.42	0.99	0.91	1.02	0.80	1.18
+3 (4/6/4/6)	-0.50	-0.14	0.80	0.74	1.31	1.22	1.36	1.15	1.52

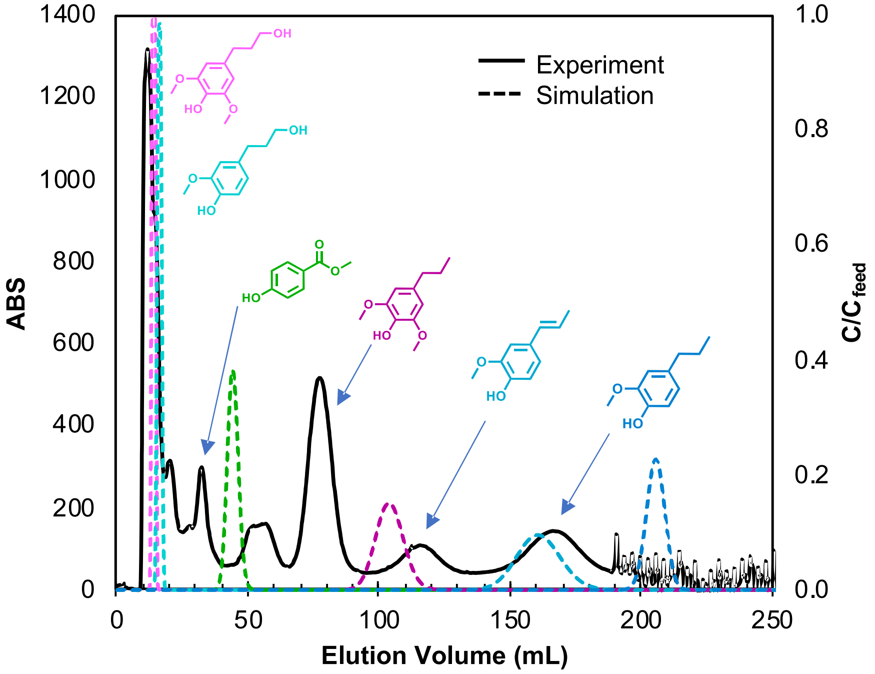

Figure S1. CUP model prediction of poplar lignin oil separation with the partition coefficients measured from shake flask tests.

Table S4. CCC operating conditions and CUP model input parameters used in this study. (EG: 4-ethylguaiacol, PG: 4-propylguaiacol, ISG: isoeugenol, P(OH)G: 4-propanolguaiacol, ES: 4-ethylsyringol, PS: 4-propylsyringol, P(ene)S: 4-propenylsyringol, P(OH)S: 4-propanolsyringol)

	Poplar (Figure 4A)	**Pine (Figure 4B)**	**Corn Stover (Figure 4C)**	**Poplar Case 1 (Figure 7A)**	**Poplar Case 2 (Figure 7B)**	**Poplar Case 3 (Figure 8)**
Column Volume (mL)	81					
Flow rate (mL)	3	3	3	15	14	15
Stationary phase retention factor (S_f)	0.885	0.885	0.885	$S_f = 0.9232-0.0163*F$ (from Figure S2)		
Column efficiency (N)	357	357	357	$N = 357.48-0.8649*F-0.2022*F^2$ (from Figure S2)		
EECCC switching volume (V_{CM}, mL)	180	180	180	46	90	95
Feed injection volume (mL)	2	2	2	6	6	6
Feed concentration (mg oil/mL)	20	20	20	103	103	200
extra-column volume (mL)	4.2	4.2	4.2	8	8	8

Feed composition and partitioning coefficient (K_P)

Poplar (Figure 4A)	Comp.	C1	P(OH)S	P(OH)G	C4	MPB	ES	P(ene)S	PS	ISG	PG	
	K_P	0.007	0.024	0.066	0.145	0.312	0.576	0.664	0.944	1.476	2.187	
Pine (Figure 4B)	Comp.	C1	P(OH)G	C3	C4	C5	C6	ISG/EG	PG			
	K_P	0.008	0.057	0.128	0.25	0.291	0.852	1.442	2.191			
Corn Stover (Figure 4C)	Comp.	P(OH)S	P(OH)G	C3	C4	MHC/ MC/ MHF/MF	ES /GA	P(ene)S	PS	EP	ISG /EG	PG
	K_P	0.036	0.082	0.17	0.254	0.342	0.601	0.656	0.94	1.271	1.474	2.199
Poplar Case 1 & 2 (Figure 7)	Comp.	C1	C2	P(OH)S	P(OH)G	MPB	ES	P(ene)S	PS	ISG	PG	
	Conc. (mg/mL)	1.947	1.545	1.030	1.030	2.915	1.380	3.605	11.629	2.379	7.488	
	K_P	0.007	0.024	0.066	0.145	0.312	0.576	0.664	0.944	1.476	2.187	
Poplar Case 3 (Figure 8)	Comp.	C1	P(OH)S	P(OH)G	C3	MPB	ES	PS	EG	PG		
	Conc. (mg/mL)	2.020	1.760	2.000	2.000	0.940	7.970	34.580	3.840	15.960		
	K_P	0	0.033	0.107	0.228	0.312	0.561	0.944	1.403	2.324		

*unknown compounds were labelled as C1-C6.

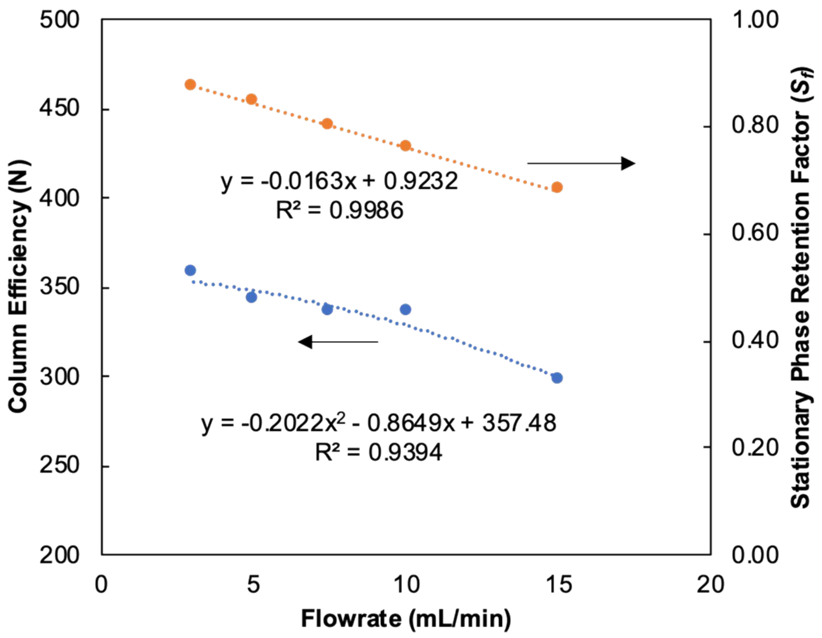

Figure S2. Correlation between flowrate and column efficiency (N), and S_f.

For simulations, the K_P values of each peak were measured from CCC data using Eq. (S1).[3]

$$K_P = \frac{(V_R - V_{MP} - V_D - 0.5V_{inj})}{V_{SP}} \quad \#(S1)$$

where V_R is the elution volume at the mass center of a peak, V_{inj} is the feed injection volume, V_D is the extra column volume, and V_{SP} and V_{MP} are the volume of the stationary and mobile phase in the column, respectively.

Table S5. The objective function used for each case study.

Case 1	Case 2
$Max\ J = Productivity\ [F, V_{CM}]$ $subject\ to\ purity \geq 99.0\%,$ $Y_{PS} \geq\ 99.0\%,$ $F \leq F_{Max}\ (= 18\ mL/min)$ $Fixed\ variables{:}C_f, V_c, V_{inj}, V_{extra}$ $Dependant\ variables{:}$ $N = 357.48 - 0.8649F - 0.2022F^2$ $S_f =\ 0.9232 - 0.0163F$	$Max\ J = Productivity\ [F, V_{CM}]$ $subject\ to\ purity \geq 99.0\%,$ $Y_i \geq\ 99.0\%\ (i = PS, ISG, PG),$ $F \leq F_{Max}\ (= 18\ mL/min)$ $Fixed\ variables{:}C_f, V_c, V_{inj}, V_{extra}$ $Dependant\ variables{:}$ $N = 357.48 - 0.8649F - 0.2022F^2$ $S_f =\ 0.9232 - 0.0163F$
Case 3	
$Max\ J = Productivity\ [F, V_{CM}]$ $subject\ to\ purity \geq 99.0\%,$ $Y_i \geq\ 99.0\%\ (i = PS, EG, PG),$ $F \leq F_{Max}\ (= 18\ mL/min)$ $Fixed\ variables{:}C_f, V_c, V_{inj}, V_{extra}$ $Dependant\ variables{:}$ $N = 357.48 - 0.8649F - 0.2022F^2$ $S_f =\ 0.9232 - 0.0163F$	

In the modeling and optimization work, the yield (Y_i), purity (P_i), and productivity (Pr_i) were defined as below.

$$Y_i = \frac{F\int_{t_1}^{t_2} C_i(t)dt}{C_{f,i}V_{inj}} \#(S2)$$

$$P_i = \frac{\int_{t_1}^{t_2} C_i(t)dt}{\sum_{j=1}^{n}\int_{t_1}^{t_2} C_j(t)dt} \#(S3)$$

$$Pr_i = \frac{Y_i C_{f,i} V_{inj}}{t_{R,n} V_c} \#(S4)$$

where $C_{f,i}$ is the feed concentration of component i, F is the flowrate, V_{inj} is the feed injection volume, V_c is the column volume, $t_{R,n}$ is the elution time for the complete elution of the last (n^{th}) component.

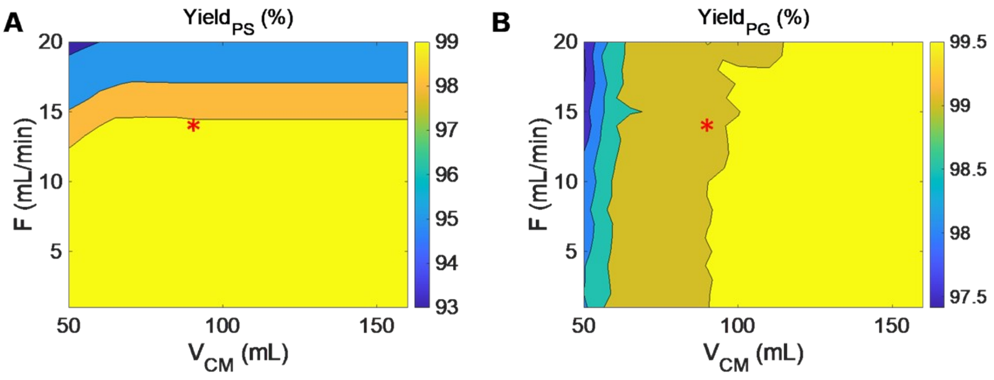

Figure S3. Contour plots of the recovery yield of (A) PS and (B) PG among various conditions in case 2.

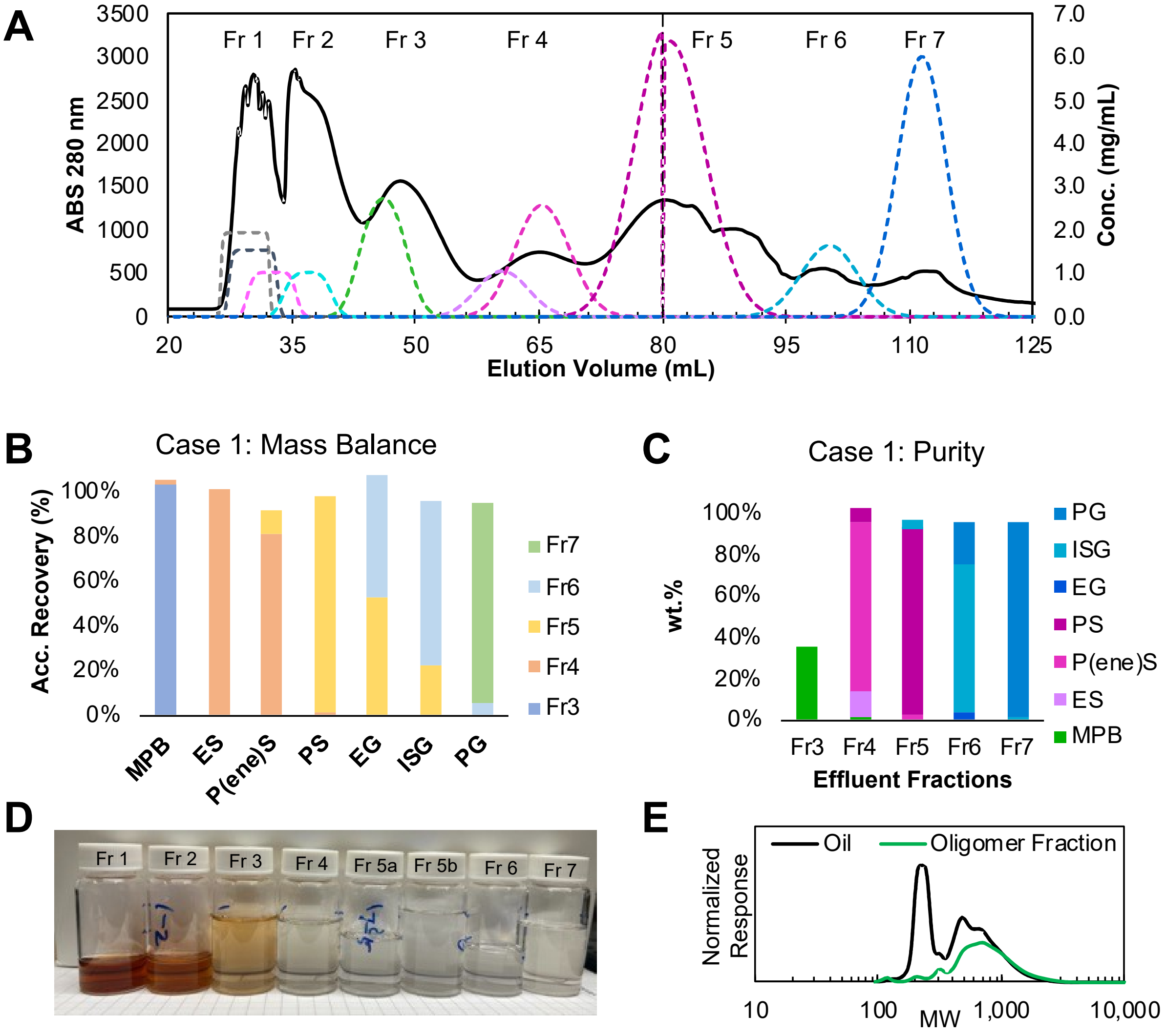

Figure S4. (A) CCC chromatogram of case 1. Effluent fractions from fraction 1 (Fr1) to fraction (Fr7) were highlighted in the chromatogram. Black solid line is UV/vis absorption data from experiment. Dashed lines are monomer concentration profiles from simulations, and the vertical dashed line indicates the stationary phase elution. (B) monomer mass balance, (C) monomer purity in effluent fractions, and (D) photos of collected effluent fractions. (MPB: methyl paraben) (E) GPC data showing comparison of lignin oil (black) to oligomeric fractions (green) Fr1 and Fr2.

Note that the recovery yield and purity of monomers were measured from collected effluent fractions based on the following equations.

$$Yield_{monomer} = \frac{C_{monomer} * V_{fraction}}{C_{f,monomer} V_{inj}} \#(S5)$$

$$Purity_{monomer} = \frac{C_{monomer} * V_{fraction}}{w_{fraction}} \#(S6)$$

where $C_{f,monomer}$ is the monomer concentration in feed, $V_{fraction}$ is the volume of effluent fraction containing the monomer, $w_{fraction}$ is the weight of the residue after evaporating solvents from the effluent fraction.

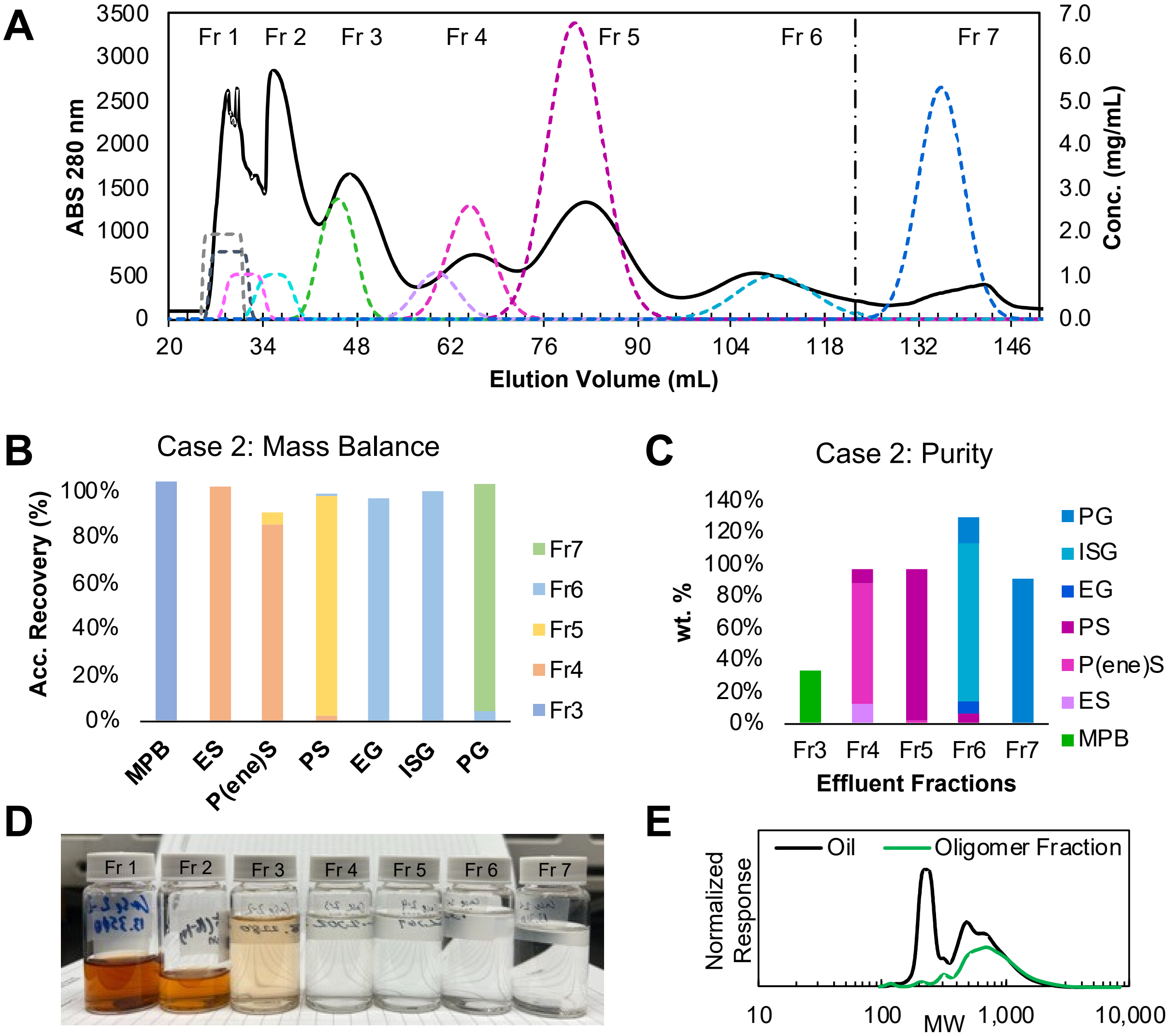

Figure S5. (A) CCC chromatogram of case 2. Effluent fractions from Fr1 to Fr7 were highlighted in the chromatogram. Black solid line is UV/vis absorption data from experiment. Dashed lines are monomer concentration profiles from simulations, and the vertical dashed line indicates the stationary phase elution. (B) monomer mass balance, (C) monomer purity in effluent fractions, and (D) photos of collected effluent fractions. (E) GPC data showing comparison of lignin oil (black) to oligomeric fractions (green) Fr1 and Fr2.

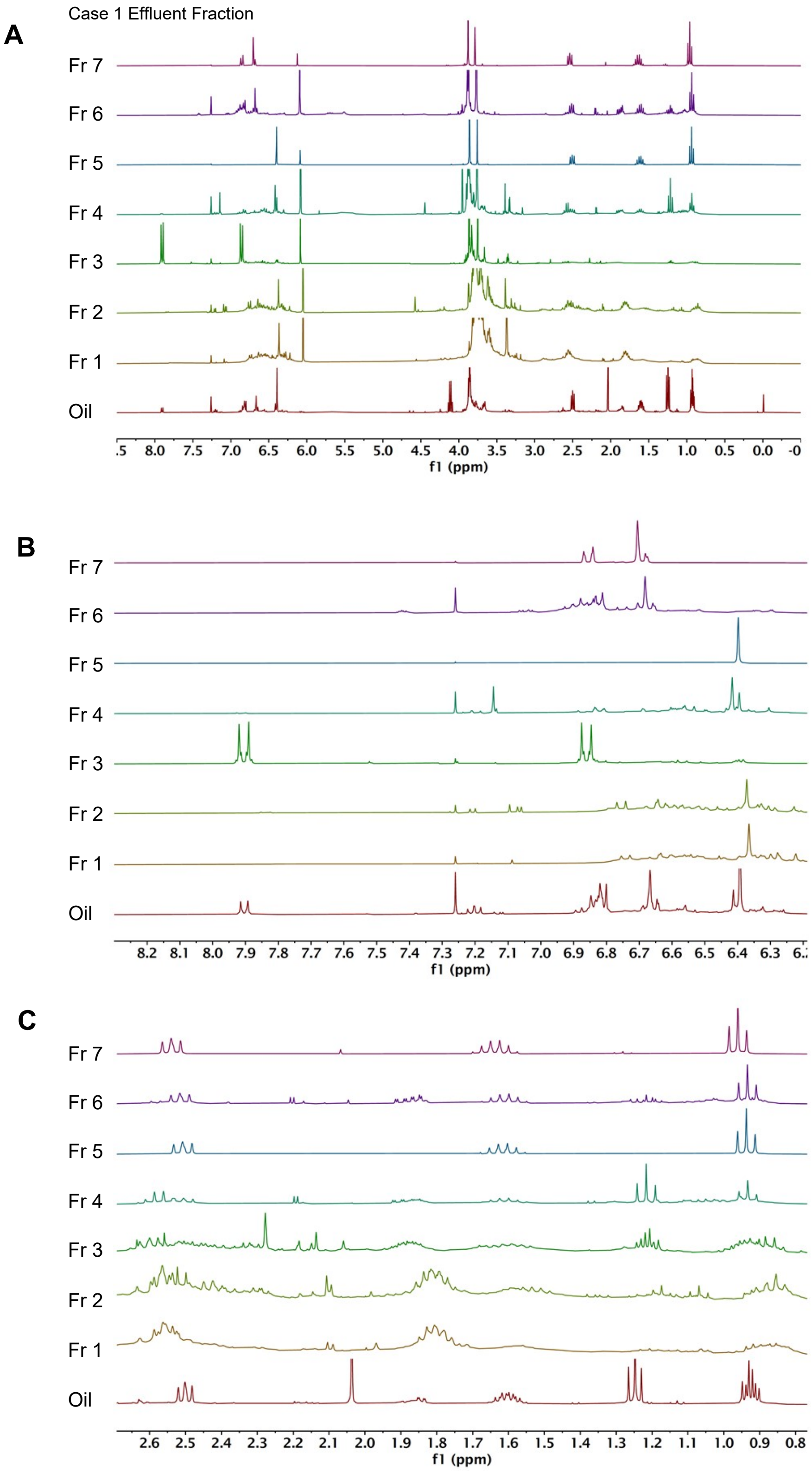

Figure S6. (A) ^{1}H-NMR spectra of RCF oil and purified monomer fractions from case 1: (A) full range from -0.5 to 8.5 ppm, (B) expansion of the aromatic region from 6.2 to 8.3 ppm, and (C) expansion of the aliphatic region from 0.75 to 2.7 ppm.

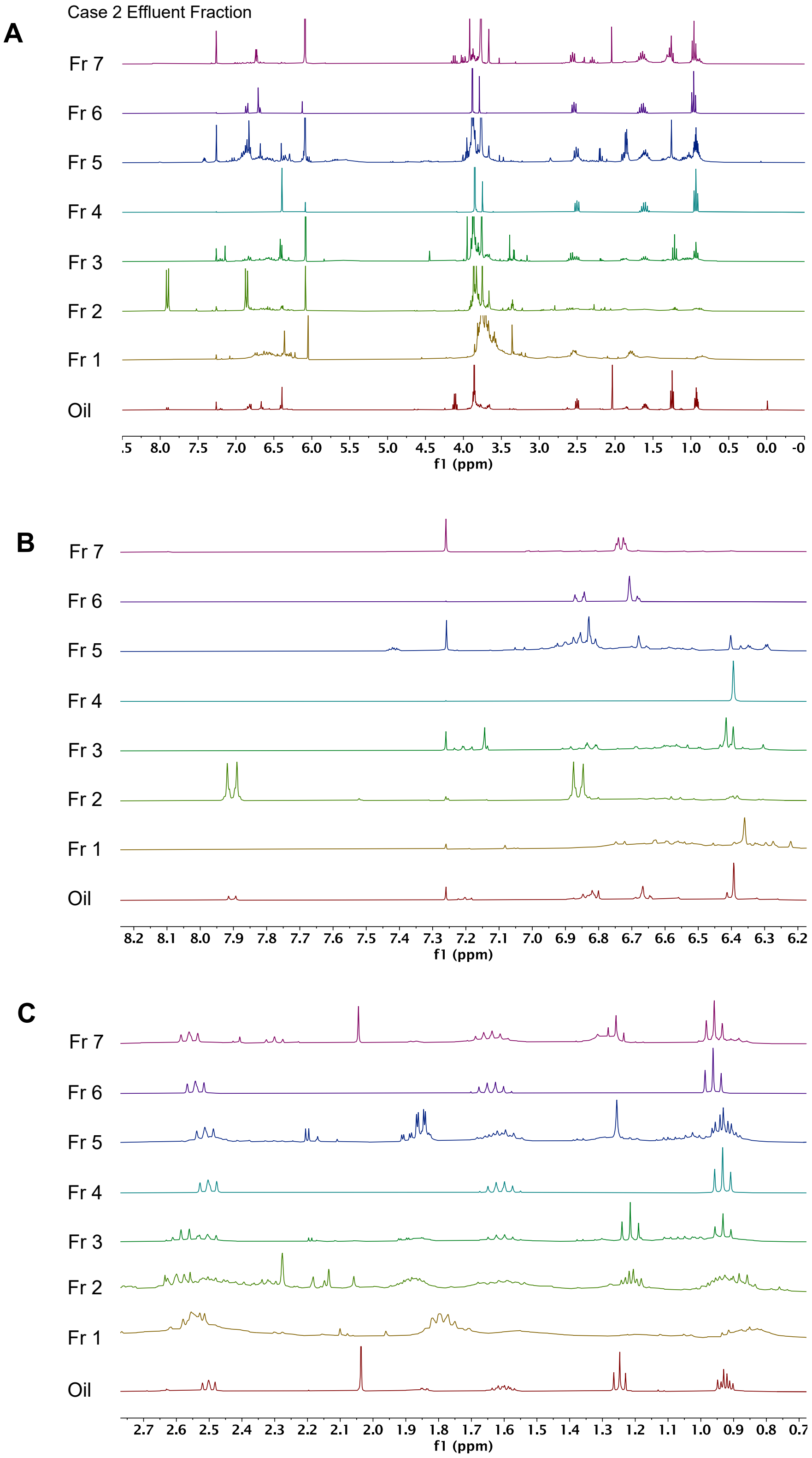

Figure S7. ^{1}H-NMR spectra of RCF oil and purified monomer fractions from case 2: (A) full range from -0.5 to 8.5 ppm, (B) expansion of the aromatic region from 6.2 to 8.25 ppm, and (C) expansion of the aliphatic region from 0.7 to 2.75 ppm.

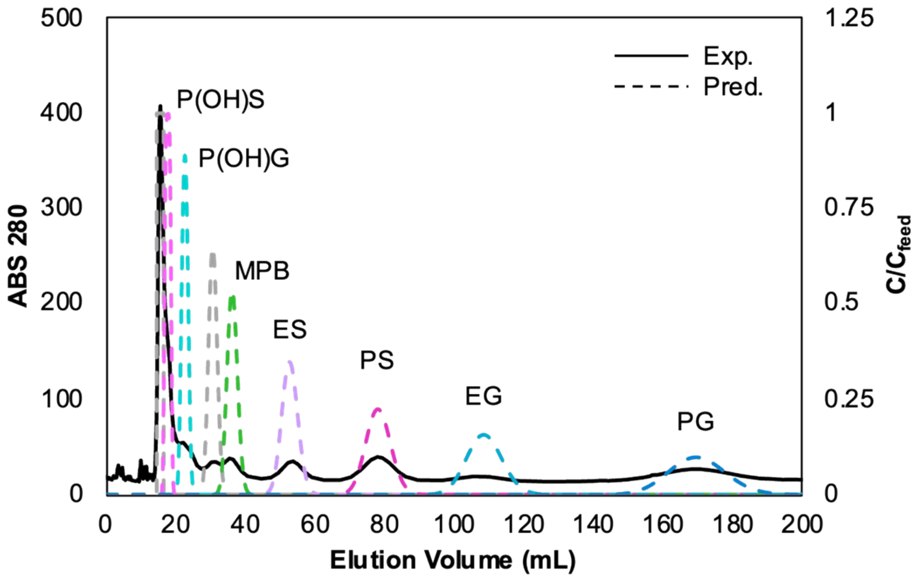

Figure S8. CCC separation of propyl-rich poplar RCF oil. Elution conditions were the same as Figure 4A. Monomers in each peak were identified by UHPLC and the partition coefficients of those monomers were measured based on the peak retention[3] and listed in Table S4.

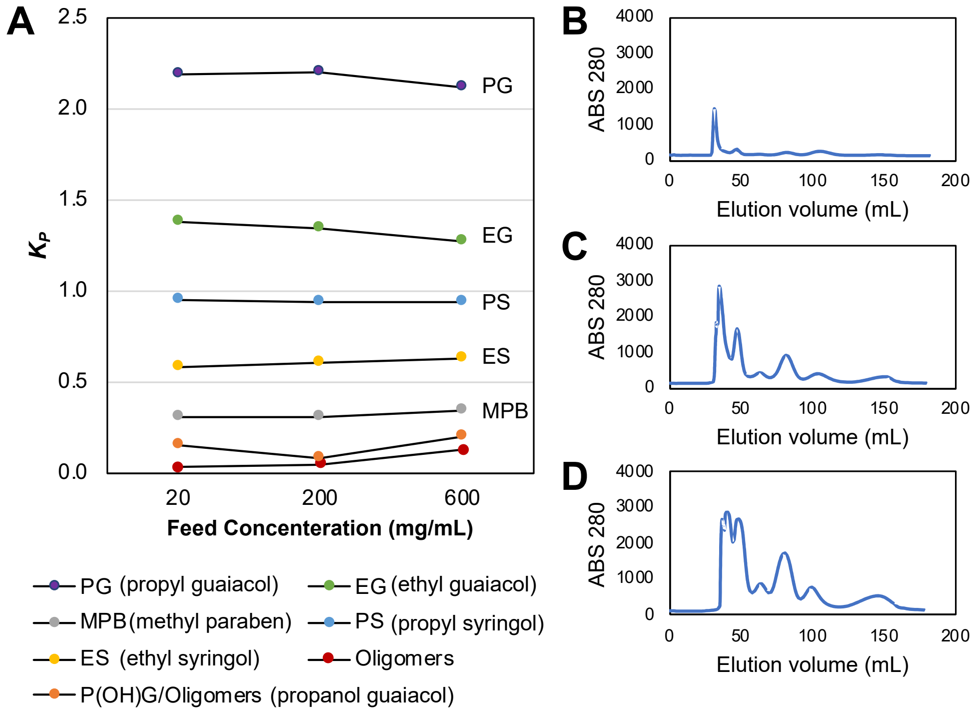

Figure S9. (A) Effect of feed concentration on the K_P of oligomers and monomers and CCC chromatogram of poplar RCF oil separations with different concentrations (B) 20 mg/mL, (C) 200 mg/mL, and (D) 600 mg/mL. The operating conditions were the same as Figure 4A except the feed concentration.

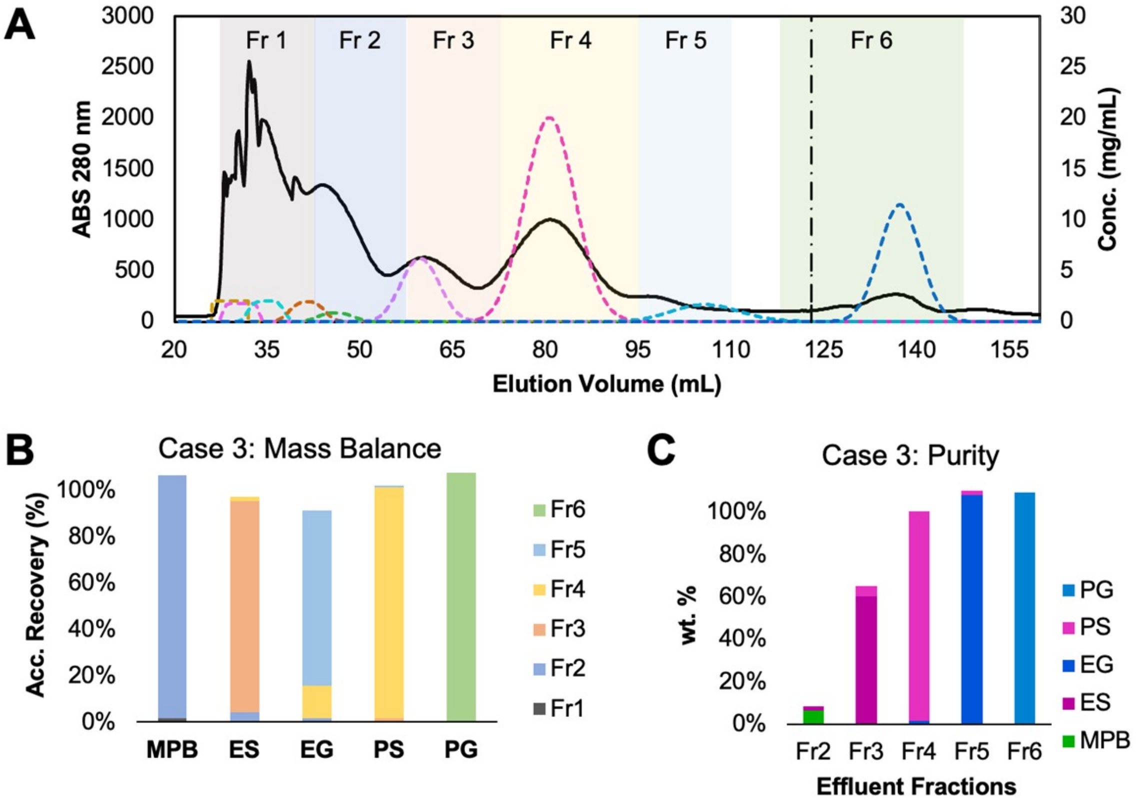

Figure S10. (A) CCC chromatogram of case 3. Effluent fractions from Fr1 to Fr6 were highlighted in the chromatogram. Black solid line is UV/vis absorption data from experiment. Dashed lines are monomer concentration profiles from simulations, and the vertical dashed line indicates the stationary phase elution. (B) monomer mass balance, and (C) monomer purity in effluent fractions.

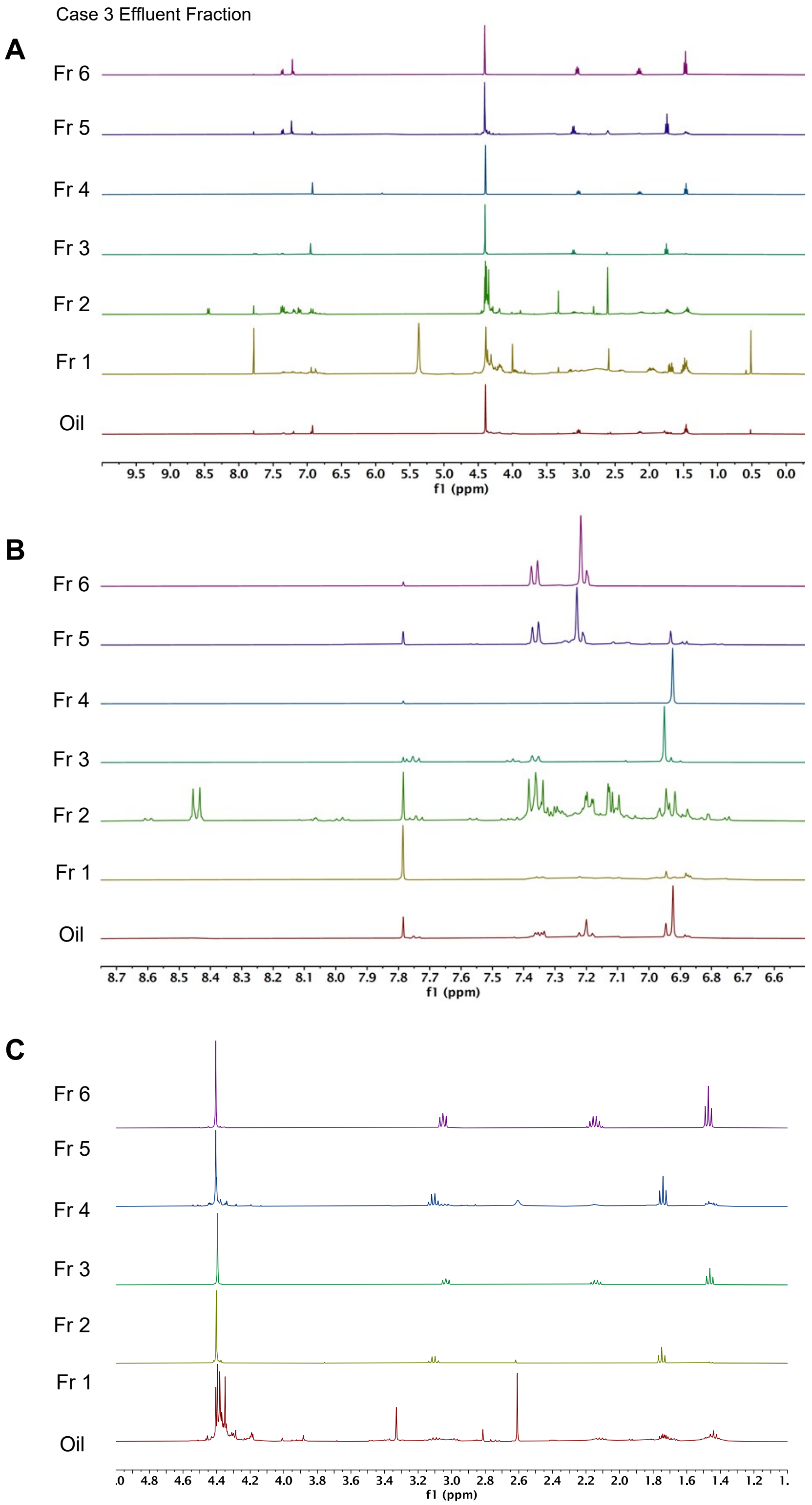

Figure S11. ^{1}H-NMR spectra of RCF oil and purified monomer fractions from case 3: (A) full range from -0.5 to 10 ppm, (B) expansion of the aromatic region from 6.5 to 8.75 ppm, and (C) expansion of the aliphatic region from 1.0 to 5.0 ppm.

References

1. J. Brent Friesen and G. F. Pauli, *Journal of Liquid Chromatography & Related Technologies*, 2005, **28**, 2777-2806.
2. A. Berthod, M. Hassoun and M. J. Ruiz-Angel, *Analytical and Bioanalytical Chemistry*, 2005, **383**, 327-340.
3. H. Choi, N. E. Soland, M. R. Moss, J. Liu, R. R. Prestangen, R. Katahira, S.-J. Lee, M. R. Thorson, C. J. Freeman and E. M. Karp, *Separation and Purification Technology*, 2022, **285**, 120330.